A Fast Approach to Near-Field Synthesis of Transmitarrays

Susana Loredo, *Senior Member, IEEE*, Germán León, and Enrique G. Plaza.

***Abstract*—We present an efficient approach to near-field synthesis of transmitarray antennas in which a planar aperture model is adopted both for the transmitarray and the field generated by it on a near plane. The necessary phases on the transmitarray are then obtained from the far field corresponding to the desired near field using simple operations such as direct and inverse fast Fourier transforms. This, together with the fact that few iterations are needed to find a valid solution, makes this approach a simple and fast alternative to near-field synthesis of this type of antennas. The proposed approach has been experimentally validated through the measurement of a manufactured prototype.**

***Index Terms*—Near-field synthesis, fast Fourier transform, transmitarray antennas, dielectric lenses.**

I. Introduction

NEAR-FIELD focusing of electromagnetic waves has received an increasing attention in recent years, due to its potential application in a number of short-range wireless systems covering different sectors, such as biomedical engineering [1], [2], non-contact microwave sensing and inspection [3], [4], radiofrequency identification (RFID) [5]-[7], or Wireless Power Transfer (WPT) [8], [9]. Moreover, both WPT and Simultaneous Wireless Information and Power Transfer (SWIPT) are receiving a lot of attention in the frame of Internet of Things (IoT) and 5G technologies [10]-[13]. Furthermore, all these applications may require complex near-field distributions including multi-focusing or shaped patterns.

In order to synthesize the excitations that originate the desired near-field radiation pattern, different approaches have been proposed in the literature [14]-[18]. These synthesis techniques often require high computation times, either because the core operation of the algorithm itself is time-consuming or because many iterations are required to converge to the optimal solution. As consequence, significant computational resources are needed if processing time is to be reduced even when acceleration techniques are implemented [19].

In this work, an algorithm is proposed to perform near-field phase-only synthesis of transmitarray antennas. The transmitarray and the spillover effect are modelled as a planar aperture from which the near field on a plane is calculated and then trimmed to the restrictions imposed on it. The necessary phases on the transmitarray are then obtained from the far field corresponding to the trimmed near field. To this end, three simple and fast operations are performed in each iteration: near-field computation (the one that takes the most time), and inverse and direct fast Fourier transform (FFT). Moreover, only a few iterations are required to find a solution, resulting in a very fast approach even in a personal computer, unlike other existing algorithms. To validate the algorithm, a 3D printed dielectric transmitarray has been manufactured and measured.

II. Near-Field Synthesis Approach

In [20], [21] a simple phase-only synthesis algorithm for the design of transmitarrays with shaped-beam far-field patterns was proposed and satisfactorily validated. That algorithm, which takes into account the spillover effect, is based on a planar aperture model [22] and the iterative application of the direct and inverse FFT [23]. In the present work, the far-field algorithm has been adapted to enable near-field synthesis with a similar philosophy, allowing FFT to continue to be used as the basic tool of the algorithm, thus maintaining the characteristics of simplicity and short time-computing. Fig. 1 shows a scheme of the near-field model, which includes the feed, the transmitarray (TA plane), and the plane where the near-field synthesis will be performed (NF plane). The power is provided by a feeding element, typically a horn, placed in the focus of the transmitarray, which actually behaves as a planar lens. The structure composed by the transmitarray itself and the radiating source is referred as the transmitarray antenna [24]. Denoting by $\vec{E}_i$ the electric field incident on *TA plane*, then E_i will refer to the $\hat{x}/\hat{y}$ field component depending on the X/Y polarization of the feed. Therefore, the incident field on a generic element (m, n) can be written as

$$E_i(x_m, y_n) = \left|E_f^{mn}\right| e^{j\phi_f^{mn}} \tag{1}$$

where the subscript *f* stands for the feed.

Transmitarray elements are modelled as isotropic punctual sources equidistant both in x and y axes, which corresponds to square unit cells. This is indeed a particular case that could be

Manuscript submitted January 20, 2021. This work was supported in part by Ministerio de Ciencia e Innovación, under project TEC2017-86619-R (ARTEINE), and by Gobierno del Principado de Asturias / FEDER under project GRUPIN-IDI-2018-000191.

S. Loredo and G. León are with the Department of Electrical Engineering, University of Oviedo, 33204 Gijón, Spain (e-mail: loredosusana@uniovi.es, gleon@uniovi.es).

E. G. Plaza is with the Department of Physics, University of Oviedo, 33204 Gijón, Spain (e-mail: gonzalezenrique@uniovi.es).

generalized to rectangular cells. To take into account the spillover radiation, the incident field from the horn will be captured both on the elements of the transmitarray itself (darker elements in Fig. 1) and also in a regular discrete mesh around it (lighter elements). The latter ones model the spillover (SP) contribution to the radiation characteristics of the transmitarray antenna. Assuming unit magnitude for the transmission coefficient, the field transmitted to the other side will be

$$E_t(x_m, y_n) = \left|E_f^{mn}\right| e^{j\phi_t^{mn}} = \begin{cases} E_i(x_m, y_n) e^{j\phi_{TA}^{mn}} & TA\ cell \\ E_i(x_m, y_n) & SP\ cell \end{cases}, \quad (2)$$

where ϕ_{TA} denotes the transmission coefficient phase.

The near field of the transmitarray antenna at each point in space can be estimated as the sum of the independent far-field contributions of each of its elements, including the spillover elements. It will be computed in a grid of *I* x *J* equally spaced locations on the plane $z = z_0$:

$$E_{NF}\left(x_i, y_j, z_0\right) = E_{NF}^{ij} = \sum_{m=1}^{M_s} \sum_{n=1}^{N_s} \frac{1}{R} E_t(x_m, y_n) e^{-jkR}, \quad (3)$$

where k is the wavenumber, and R the distance between the element (m, n) and the location where the near field is being calculated.

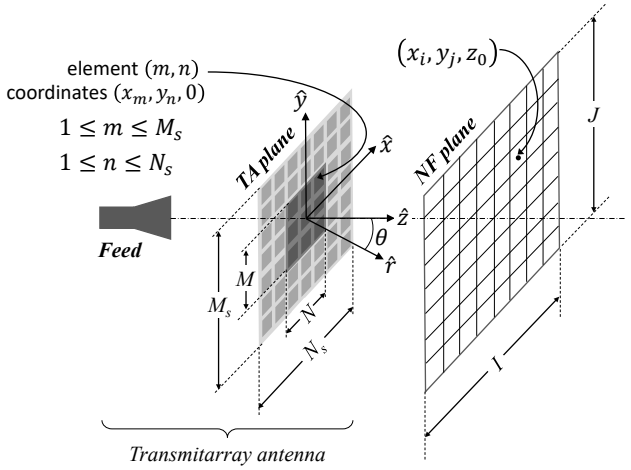

Fig. 1. Scheme of the transmitarray system.

The goal of the algorithm will be to find the necessary phases ϕ_{TA}^{mn} to achieve a near-field pattern at the plane $z = z_0$ that satisfy the given specifications, which may include pointing direction, beamwidth in the main cuts, amplitude ripple, and secondary lobe level (SLL). From these specifications, upper ($T_{up}(x, y)$) and lower ($T_{low}(x, y)$) auxiliary templates will be defined. Since the objective is not to strictly comply with templates but only with the initial specifications, the templates might be adjusted during the execution of the algorithm to facilitate convergence.

Fig. 2 shows the flowchart of the proposed algorithm. The synthesis procedure starts by initializing the transmitted field (E_{t0}) to the value of the incident field. Then, the near field (E_{NF}) is computed and compared to the defined templates, giving place to a modified near field (E_{NFmod}):

$$|E_{NFmod}| = \begin{cases} \frac{1}{\sqrt{2}} T_{up}(x, y), & |E_{NF}| > T_{up}(x, y) \\ \sqrt{T_{low}(x, y)}, & |E_{NF}| < T_{low}(x, y) \\ |E_{NF}|, & otherwise. \end{cases} \quad (4)$$

This will imply a new transmitted field (E_t), which will be obtained as follows. The radiation pattern due to the modified near-field aperture (RP_{NFmod}) is obtained through a 2-D inverse FFT of $K \times K$ points, with $K > M_s, N_s$. From this, the radiation pattern due to the new transmitarray (RP_{TAnew}) is estimated as:

$$RP_{TAnew} \approx RP_{NFmod} \cdot exp\left(j(\angle RP_{TA} - \angle RP_{NF})\right), \quad (5)$$

being RP_{TA} and RP_{NF} the radiation patterns due to the transmitarray and near-field aperture respectively before modifying the near field. This approach is based on the finding that $|RP_{NF}| \approx |RP_{TA}|$. Thus, the same is assumed for the relation between $|RP_{NFmod}|$ and $|RP_{TAnew}|$, assuming also that the phase difference between RP_{NF} and RP_{TA} holds between RP_{NFmod} and RP_{TAnew}. This has proven to be a reasonably approach, leading to satisfactory results, as will be shown in Section III.

Applying now a 2D FFT the necessary transmitted field is retrieved. It is a $K \times K$ matrix, from which extra elements must be removed to fit its size to that of the transmitarray, including the spillover elements. Then, the amplitude of the transmitted field is restored to that of the incident field, and also the phase of the spillover elements. Finally, the near field due to this new transmitted field is obtained, repeating iteratively the process until specifications are met or the maximum number of iterations is reached.

III. Results and Validation

Two different results will be presented to illustrate and validate the proposed algorithm. In the first one, a transmitarray will be synthesized to focus the energy on two close points in given directions, whereas in the second one a planar amplitude in one of the near-field cuts will be desired. Furthermore, in this case the synthesized phases will be used to fabricate a *quasi-planar* dielectric transmitarray, which will be measured in a near-field planar range. The working frequency will be 28 GHz in both cases, and the periodicity of the cells $0.3\lambda \times 0.3\lambda$. The transmitarray will be square, i.e. $M = N$, and also $M_s = N_s$. The incident field will be estimated using the NFPC (Near-Field Plane Cuts) model presented in [22] and also used in [21].

A. Case 1: Two foci

For this case, two simultaneous foci are generated at $\theta = \pm 30°$. The spot width must be approximately λ on the plane $z = 0.5D$, being *D* the length of the transmitarray side, and the field level outside the desired beams should be less than -10 dB.

A transmitarray of 40×40 cells was chosen. The algorithm was executed with $M_s = N_s = 80$, i.e. 4800 spillover elements were uniformly distributed around the transmitarray, as indicated in Fig. 1. The maximum number of iterations was

fixed to ten, and auxiliary templates were defined to drive the results to compliance with specifications. The near-field grid consisted of 100489 points (317×317) sampled each 0.15λ. After running the loop of Fig. 2 all ten times, the best result was found for four iterations. The general criterion for choosing the best result is that the percentage of near-field samples that do not comply with the templates is the lowest. In this case, that percentage was 0.096%. This whole process took 5.41 minutes in a laptop Intel Core i5-8265U with 8 GB DDR4 memory.

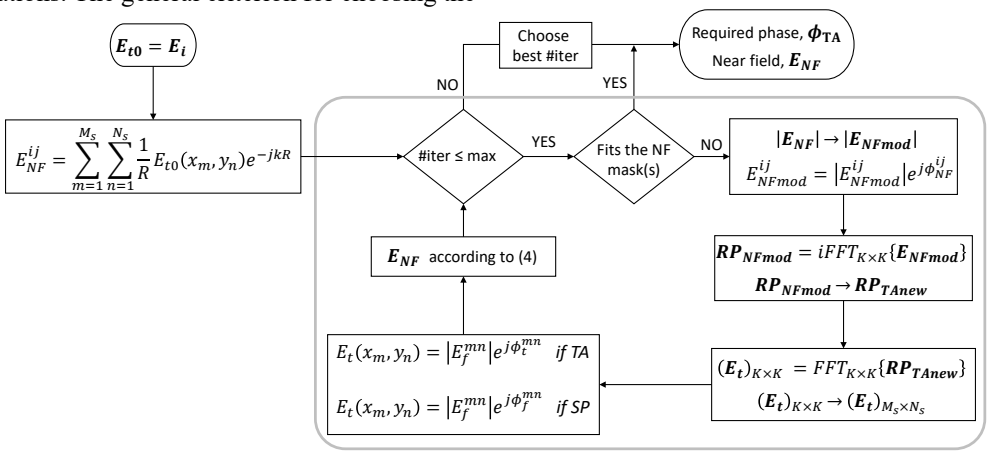

Fig. 2. Flowchart of the near-field synthesis algorithm.

Fig. 3 shows the synthesized phases for the transmission coefficient. Fig. 4 shows the near field achieved both on the plane $z = 0.5D$ (Fig. 4(a)) and the plane $y = 0$ (Fig. 4(b)). In both figures the amplitude is normalized to its maximum value. On *NF plane*, the maximum values of the field take place exactly at the expected positions ($x = \pm 45\ mm$, $y = 0$), and the level at other directions is kept under -10 dB, as can be appreciated in Fig. 4(a).

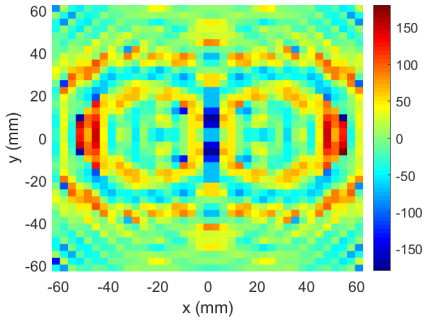

Fig. 3. Case 1: synthesized phases.

B. *Case 2: Beamforming*

Now a planar amplitude along x axis is desired, which will be specified by a -3dB beamwidth on the plane $z = D$ of approximately 9.5λ (x) × 2λ (y), amplitude ripple of 1.5 dB, and SLL under -10 dB. Furthermore, the result will be applied to the design of a dielectric transmitarray, that is an array where the unit cell is a dielectric slab and phase tuning is achieved by varying the slab height in the different cells that make up the array [25]. In order to have a transmitarray as planar as possible, that corresponds to the planar aperture model, the phase range will be limited to 240 degrees instead of the whole 360-degree range [21].

The results are shown in Fig. 5 to Fig. 8 for a transmitarray of 36×36 elements ($M_s = N_s = 72$), a near-field grid of 81225 points, and seven iterations of the algorithm. In this case, the execution time was 3.74 minutes in the same computer. Fig. 5 shows both the synthesized phase distribution and the fabricated dielectric lens. Both the lens and the mechanical support used to attach it to the horn were fabricated with a general-purpose 3D printer, with fundamental resolution of $100\ \mu m$. The dielectric material was polylactic acid (PLA) with $\varepsilon_r = 2.5$ and $tan\delta = 0.005$. The near field was measured in the planar range described in [26].

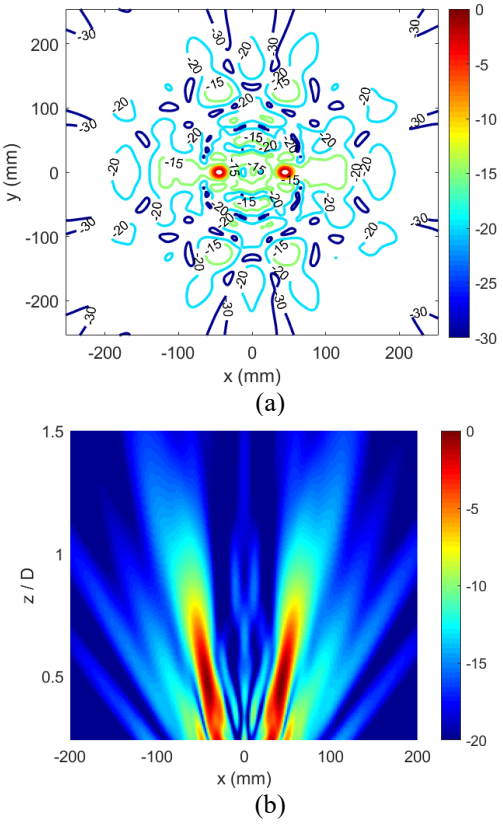

Fig. 4. Case 1: Near-field amplitude at (a) plane $z = 0.5D$ (NF plane); (b) plane $y = 0$.

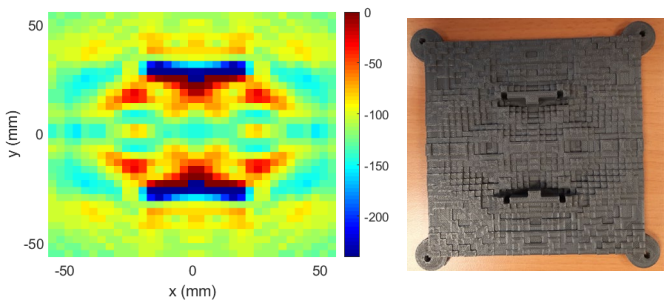

(a) (b)

Fig. 5. Case 2: (a) Synthesized phases (degrees); (b) Fabricated lens.

In Fig. 6 the near-field amplitude resulting from the algorithm is compared with that measured for the fabricated transmitarray, and Fig. 7 compares the main cuts of the measured near-field amplitude with the results given by the model. A photograph taken during the measurement process is also included. The auxiliary templates used in the algorithm are included for comparison purposes, and also the -3dB line. The beamwidth at this level is $9.3\lambda \times 2\lambda$ both for the model and the measurement, thus meeting the requirement. Moreover, the agreement is good not only along the main cuts (Fig. 7), but also on the whole plane, as can be observed in Fig. 6. It should be emphasized that the templates are auxiliary tools that are intended to make the near-field pattern comply with the initial specifications, for which it is not strictly necessary that it be completely adjusted to them. In this case, the percentage of positions that did not comply with the templates was 0.3%. Finally, Table I compares this approach with some of the algorithms found in the literature.

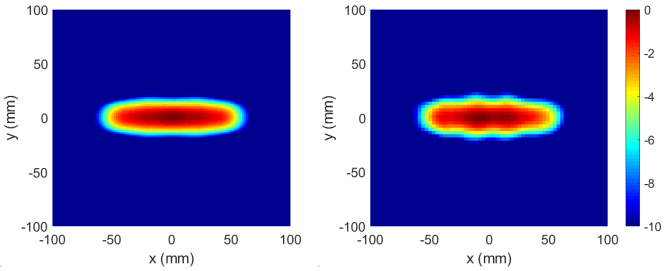

(a) (b)

Fig. 6. Case 2: Near-field amplitude at plane $z = D$: (a) from model; (b) from measurements.

IV. Conclusion

In this paper, an efficient approach has been proposed to perform near-field synthesis of transmitarray antennas. This approach consists of designing the transmitarray based on the far field corresponding to a desired near field. Its main advantages are its simplicity, since it is mainly based on FFT, and its short computing time, since the operations involved are not time consuming and in addition a few iterations are enough to find a result that meets the required specifications. This makes it possible for it to run on a standard personal computer in a few minutes.

Although the algorithm is based on a planar aperture model, its results can also be applied to the design of *quasi-planar* dielectric lenses or transmitarrays, which was the option chosen to experimentally validate the algorithm due to its manufacturing simplicity. The measurement of the prototype has served to demonstrate the viability of the proposal. Furthermore, this approach can also be extended to other array antennas with either phase-only or amplitude and phase synthesis.

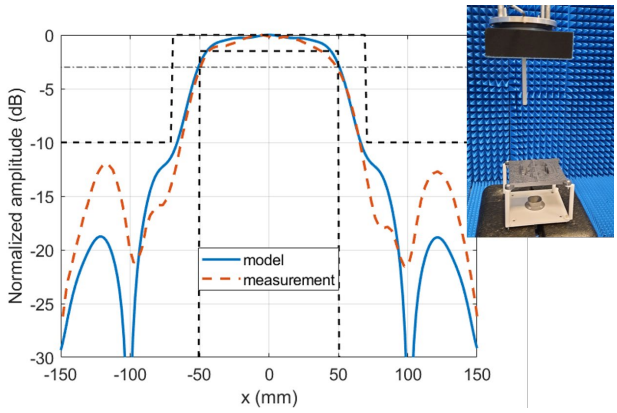

(a)

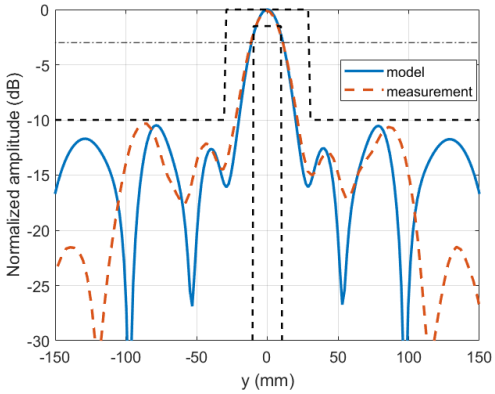

(b)

Fig. 7. Case 2: Near-field amplitude for the plane $z = D$. Comparison of model results and measurements: (a) cut $y = 0$, and prototype in the measurement planar escanner; (b) cut $x = 0$.

TABLE I
Comparison of Algorithms

Ref.	Description	NF constraints	Algorithm	Computing time / Resources
[17]	Only focusing applications	Location of focal points	-	-
[18]	Source array of 20402 elements; 15136 NF values	Target distribution of NF intensities	Dyadic Green's function	78 hours / PC with 2 Intel E5-2687W v2 CPU; 256 GB memory
[19]	Reflectarray of 1080 elements; NF grid of 6561 points; 2 NF planes	Templates	Intersection Approach	10.3 days / Workstation Intel Xeon E5-2630 v4 CPU at 2.2 GHz; 10 cores, 20 threads
			Differential contributions	12.5 min. / the same above
This paper	Array of 6400 elements (TA+SP) NF grid of 100489 points	Pointing direction(s), beamwidth, ripple, SLL	FFT	6 min / laptop Intel Core i5-8265U; 8 GB DDR4 memory

REFERENCES

[1] F. Tofigh, J. Nourinia, M. Azarmanesh, and K. M. Khazaei, "Near-field focused array microstrip planar antenna for medical applications", *IEEE Antennas Wireless Propag. Lett.*, vol. 13, pp. 951–954, May 2014.

[2] X. He, W. Geyi, and S. Wang, "Optimal design of focused arrays for microwave-induced hyperthermia", *IET Microwaves, Antennas Propag.*, vol. 9, no. 14, pp. 1605-1611, 2015.

[3] K. D. Stephan, J. B. Mead, D. M. Pozar, L. Wang, and J. A. Pearce, "A near-field focused microstrip array for a radiometric temperature sensor", *IEEE Trans. Antennas Propag.*, vol. 55, no. 4, pp. 1199-1203, Apr. 2007.

[4] M. Bogosanovic and A. G. Williamson, "Microstrip antenna array with a beam focused in the near-field zone for application in noncontact microwave industrial inspection", *IEEE Trans. Instrum. Meas.*, vol. 56, no. 6, pp. 2186-2195, Dec. 2007.

[5] A. Buffi, A. A. Serra, P. Nepa, H-.T. Chou, and G. Manara, "A focused planar microstrip array for 2.4 GHz RFID readers", *IEEE Trans. Antennas Propag.*, vol. 58, no. 5, pp. 1536-1544, May 2010.

[6] H.-T. Chou, T.-M. Hung, N.-N. Wang, H.-H. Chou, C. Tung, and P. Nepa, "Design of a near-field focused reflectarray antenna for 2.4 GHz RFID reader applications", *IEEE Trans. Antennas Propag.*, vol. 59, no. 3, pp. 1013-1018, March 2011.

[7] H.-T. Chou, M. Y. Lee, and C. T. Yu, "Subsystem of phased array antennas with adaptive beam steering in the near-field RFID applications", *IEEE Antennas Wireless Propag. Lett.*, vol. 14, pp. 1476-1479, 2015.

[8] V. R. Gowda, O. Yurduseven, G. Lipworth, T. Zupan, M. S. Reynolds, and D. R. Smith, "Wireless power transfer in the radiative near-field", *IEEE Antennas Wireless Propag. Lett.*, vol. 15, pp. 1865-1868, 2016.

[9] B. J. DeLong, A. Kiourti, and J. L. Volakis , "A radiating near-field patch rectenna for wireless power transfer to medical implants at 2.4 GHz", *IEEE J. Electromagn., RF, Microw. Med. Biol.*, vol. 2, no. 1, pp. 64-69, March 2018.

[10] T. D. P. Perera, D. N. K. Jayakody, S. Chatzinotas, and V. Sharma, "Wireless information and power transfer: issues, advances, and challenges", in *Proc. VTC-Fall*, Toronto, ON, Canada, 2017.

[11] M. Molefi, E. D. Markus, and A. Abu-Mahfouz, "Wireless power transfer for IoT devices - a review", in *Proc. IMITEC*, Vanderbijlpark, South Africa, 2019.

[12] D. S. Gurjar, H. H. Nguyen, and H. D. Tuan, "Wireless information and power transfer for IoT applications in overlay cognitive radio networks", *IEEE Internet Things J.*, vol. 6, no. 2, pp. 3257-3270, Apr. 2019.

[13] D. Zhai, R. Zhang, J. Du, Z. Ding, and F. R. Yu, "Simultaneous wireless information and power transfer at 5G new frequencies: channel measurement and network design", *IEEE J. Sel. Areas Commun.*, vol. 37, no. 1, pp. 171-186, Jan. 2019.

[14] H.-T. Chou, N. N. Wang, H. H. Chou, and J. H. Qiu, "An effective synthesis of planar array antennas for producing near-field contoured patterns", *IEEE Trans. Antennas Propag.*, vol. 59, no. 9, pp. 3224-3233, Sep. 2011.

[15] S. Clauzier, S. M. Mikki, and Y. M. M. Antar, "Design of near-field synthesis arrays through global optimization", *IEEE Trans. Antennas Propag.*, vol. 63, no. 1, pp. 151-165. Jan. 2015.

[16] A. F. Vaquero, D. R. Prado, M. Arrebola, M. R. Pino, and F. Las-Heras, "Near-field synthesis of reflectarrays using intersection approach", in *Proc. EUCAP*, Paris, France, 2017, pp. 3644-3648.

[17] S. Yu, H. Liu, and L. Li, "Design of near-field focused metasurface for high-efficient wireless power transfer with multifocus characteristics", *IEEE Trans. Ind. Electron.*, vol. 66, no. 5, pp. 3993-4002, May 2019.

[18] J. W. Wu, R. Y. Wu, X. C. Bo, L. Bao, X. J. Fu, and T. J. Cui, "Synthesis algorithm for near-field power pattern control and its experimental verification via metasurfaces", *IEEE Trans. Antennas Propag.*, vol. 67, no. 2, pp. 1073-1083, Feb. 2019.

[19] D. R. Prado, A. F. Vaquero, M. Arrebola, M. R. Pino, and F. Las-Heras, "Acceleration of gradient-based algorithms for array antenna synthesis with far-field or near-field constraints", *IEEE Trans. Antennas Propag.*, vol. 66, no. 10, pp. 5239-5248, Oct. 2018.

[20] S. Loredo, G. León, O. F. Robledo, and E. G. Plaza, "Phase-only synthesis algorithm for transmitarrays and dielectric lenses", *ACES J.*, vol. 33, no. 3, pp. 259-264, March 2018.

[21] S. Loredo and G. León, "Synthesis algorithm for "quasi-planar" dielectric lenses", in *Proc. EuCAP*, Krakow, Poland, 2019.

[22] E. G. Plaza, G. León, S. Loredo, and F. Las-Heras, "A simple model for analyzing transmitarray lenses", *IEEE Antennas Propag. Mag*., vol. 57, no. 2, pp. 131-144, Apr. 2015.

[23] W. P. M. N. Keizer, "Fast low-sidelobe synthesis for large planar array antennas utilizing successive fast Fourier transfoms of the array factor", *IEEE Trans. Antennas Propag*., vol. 65, no. 2, pp. 529-540, Feb. 2017.

[24] J. R. Reis, M. Vala, R. P. S. Caldeirinha, "Review paper on transmitarray antennas", *IEEE Access*, vol. 7, pp. 94171-94188, 2019.

[25] P. Nayeri, M. Liang, R. A. Sabory-García, M. Tuo, F. Yang, M. Gehm, H. Xin, and A. Z. Elsherbeni, "3D printed dielectric reflectarrays: low-cost high-gain antennas at sub-millimeter waves", *IEEE Trans. Antennas Propag*., vol. 62, no. 4, pp. 2000-2008, Apr. 2014.

[26] A. Arboleya, Y. Álvarez, and F. Las-Heras, "Millimeter and submillimeter planar measurement setup", in *Proc. APSURSI*, Orlando, FL, USA, 2013.